Supplementary Information

Building Porphyrin-Based MOF on MXene for ppb-Level NO Sensing

*Yanwei Chang[1, 2], Minyi Chen[1, 2], Zijing Fu[1, 2], Ruofei Lu[1, 2], Yixun Gao[1, 2], Fengjia Chen[3, 4], Hao Li[1, 2], Nicolaas Frans de Rooij[2], Yi-Kuen Lee[5, 6], Yao Wang[1, 2] *, and Guofu Zhou[1, 2]*

[1]Guangdong Provincial Key Laboratory of Optical Information Materials and Technology, Institute of Electronic Paper Displays, South China Academy of Advanced Optoelectronics, South China Normal University, Guangzhou 510006, P. R. China.
[2]National Center for International Research on Green Optoelectronics, South China Normal University, Guangzhou 510006, P. R. China.
[3]Division of Pulmonary and Critical Care Medicine, The First Affiliated Hospital of Sun Yat-sen University, Guangzhou 510006, P. R. China.
[4]Institute of Pulmonary Diseases, Sun Yat-sen University, Guangzhou 510006, P. R. China.
[5]Department of Mechanical & Aerospace Engineering, Hong Kong University of Science and Technology, Clear Water Bay, Kowloon, Hong Kong Special Administrative Region.
[6]Department of Electronic & Computer Engineering, Hong Kong University of Science and Technology, Clear Water Bay, Kowloon, Hong Kong Special Administrative Region.

** Corresponding Author: Yao Wang, Email: wangyao@m.scnu.edu.cn*

Table of contents

S1. TEM image of $Ti_3C_2T_x$

Figure S1 demonstrated $Ti_3C_2T_x$ was a typical 2D layered structure.

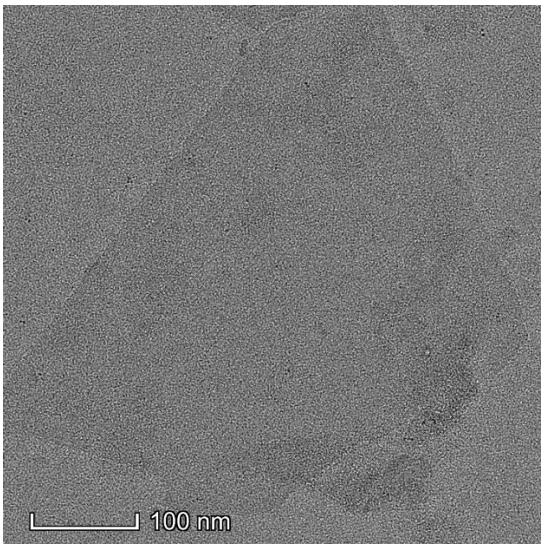

Figure S1. TEM image of $Ti_3C_2T_x$.

S2. AFM image of $Ti_3C_2T_x$

AFM tapping mode investigation indicated that the average thickness of $Ti_3C_2T_x$ nanosheets was around 2.02 nm with a standard deviation of 0.51 nm.

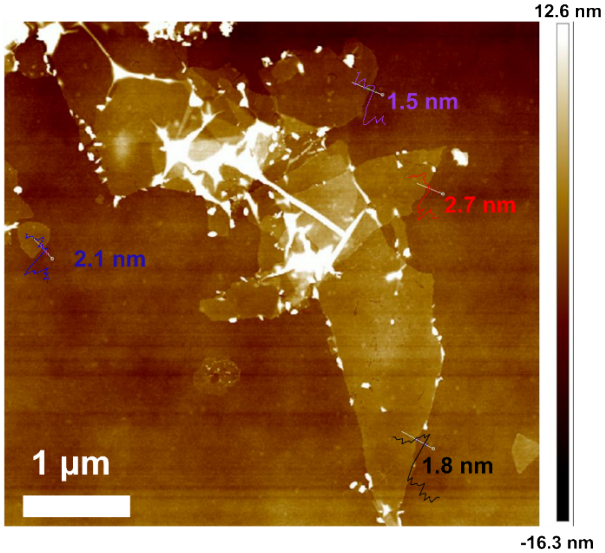

Figure S2. AFM image (tapping mode) of $Ti_3C_2T_x$.

S3. XPS spectra of $Ti_3C_2T_x$, Co-TCPP(Fe) and Co-TCPP(Fe)/$Ti_3C_2T_x$-20

The XPS survey spectra of $Ti_3C_2T_x$, Co-TCPP(Fe) and Co-TCPP(Fe)/$Ti_3C_2T_x$-20 were demonstrated in Figure S3. The high-resolution spectra of C 1s of $Ti_3C_2T_x$, Co-TCPP(Fe) and Co-TCPP(Fe)/$Ti_3C_2T_x$-20 were shown in Figure S3b. For $Ti_3C_2T_x$, the five peaks of $Ti_3C_2T_x$ showed at 281.7 eV, 282.5 eV, 284.8eV, 286.3 eV and 289.3 eV were attributed to C-Ti-Tx(C-Ti-O), C-Ti-Tx(C-Ti-OH), C-C, C-O and C=O/C-F, respectively.[61]

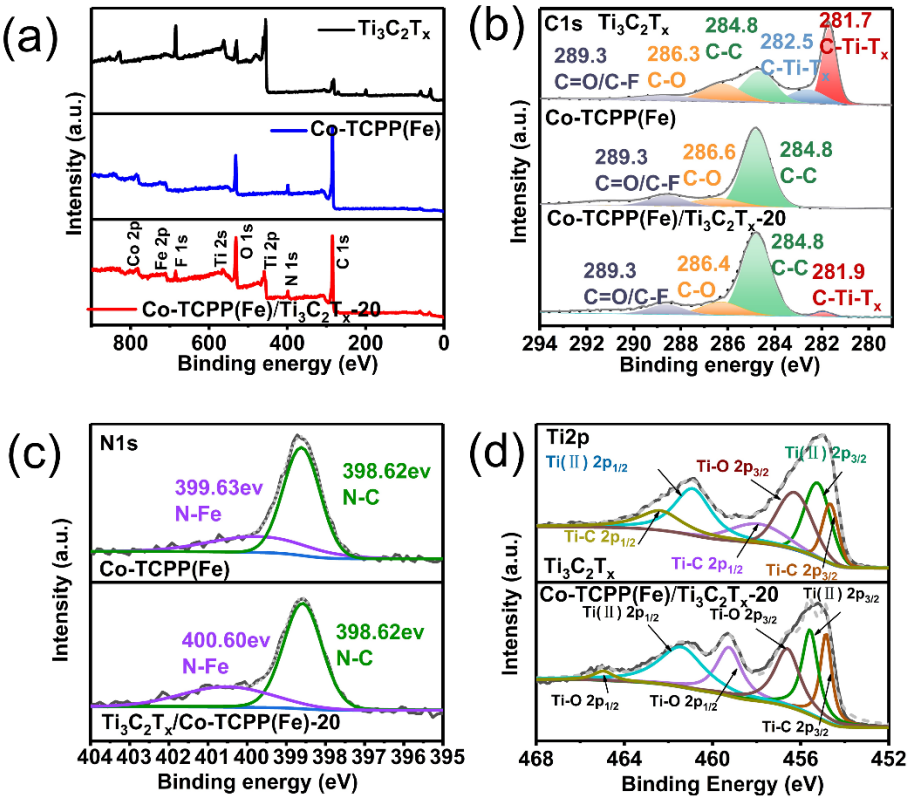

Figure S3. XPS spectra (a) and high-resolution spectra of C 1s (b) of $Ti_3C_2T_x$, Co-TCPP(Fe) and Co-TCPP(Fe)/$Ti_3C_2T_x$-20. (c) High-resolution spectra of N 1s of Co-TCPP(Fe) and Co-TCPP(Fe)/$Ti_3C_2T_x$-20. (d) High-resolution spectra of Ti 2p of $Ti_3C_2T_x$ and $Ti_3C_2T_x$/Co-TCPP(Fe)-20.

Furthermore, the XPS spectra of C 1s of Co-TCPP(Fe) showed three peaks corresponding to C–C, C–O and C=O groups at 284.8 eV, 286.4 eV and 289.3 eV, respectively.[61] The reduction of characteristic peaks of C 1s at 281.9 eV in the XPS

spectra of Co-TCPP(Fe)/$Ti_3C_2T_x$ -20 confirmed that the groups of C-Ti-O and C-Ti-OH on the surface of $Ti_3C_2T_x$ changed after assembly with Co-TCPP(Fe). Figure S3c showed the N-Fe peak of Co-TCPP(Fe) and Co-TCPP(Fe)/$Ti_3C_2T_x$-20. The peaks of Co-TCPP(Fe)/$Ti_3C_2T_x$-20 were positively shift compared with Co-TCPP(Fe), verifying the charge transfer between $Ti_3C_2T_x$ and Co-TCPP(Fe).[65] In the Figure S3d, the spectra of Ti 2p of $Ti_3C_2T_x$ and Co-TCPP(Fe)/$Ti_3C_2T_x$-20 were consistent with the reported values. [66]

S4. Raman spectra of $Ti_3C_2T_x$, Co-TCPP(Fe) and Co-TCPP(Fe)/$Ti_3C_2T_x$-20

Raman spectra were exhibited to analyze the chemical structure and affirm the hydrogen bond interaction between $Ti_3C_2T_x$ and Co-TCPP(Fe) in Figure S4. In the range of 100-800 cm^{-1}, Co-TCPP(Fe)/$Ti_3C_2T_x$-20 hybrid contained the whole characteristic peaks of $Ti_3C_2T_x$ (Figure S4b). Firstly, the bands at 712 cm^{-1} (ω_3) and 195 cm^{-1} (ω_2) were ascribed to the A_{1g} symmetric out-of-plane vibrations of C atom and Ti atom, respectively. Besides, the bands at 619 cm^{-1} (ω_4), 381 cm^{-1} (ω_5), and 270 cm^{-1} (ω_5) belonged to the E_g group vibrations, mainly consisting of in-plane shearing modes of C, Ti, and other surface terminal atoms.[60]

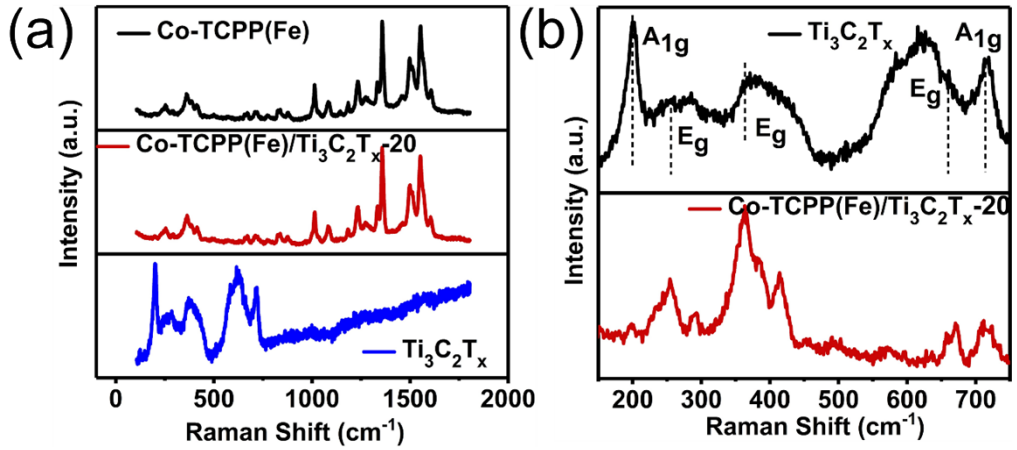

Figure S4 (a) Raman spectra of Co-TCPP(Fe), Co-TCPP(Fe)/$Ti_3C_2T_x$-20 and $Ti_3C_2T_x$. (b) High-resolution Raman spectra of $Ti_3C_2T_x$ and Co-TCPP(Fe)/$Ti_3C_2T_x$-20.

S5. Humidity resistance test of Co-TCPP(Fe)/$Ti_3C_2T_x$-20 based sensor

The gas sensing responses of Co-TCPP(Fe)/$Ti_3C_2T_x$ based sensor in the different R.H of 0%, 30%, 50%, and 70% were shown in Figure S5. It was found that Co-TCPP(Fe)/$Ti_3C_2T_X$ based sensor exhibited response decreasing along with the increase of R.H., which was attributed to the competition between the H_2O and NO molecules adsorbed on the surface of the sensing layer. It is indicated that the obtained sensor is not resistant to humidity. This issue could be addressed by the matured technology of pre-drying the injected exhaled breath.

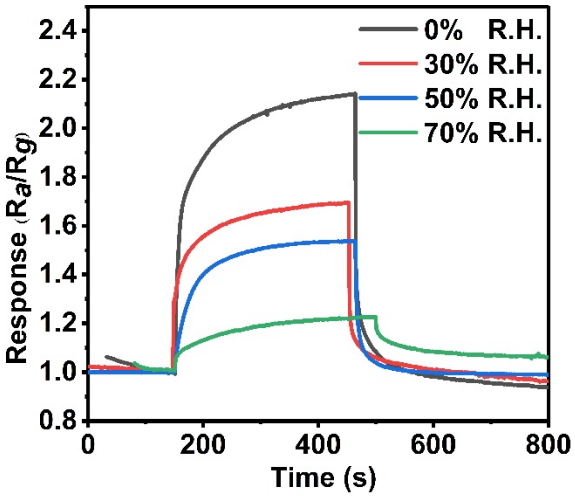

Figure S5 Gas sensing responses of Co-TCPP(Fe)/$Ti_3C_2T_x$-20 based sensor toward 10 ppm NO under different relative humidity at room temperature.

S6. Control system of Co-TCPP

S6.1 The Synthesis of Co-TCPP

TCPP (8.6 mg, 0.011 mmol), $Co(NO_3)_2 \cdot 6H_2O$ (12.8 mg, 0.044 mmol) and 1.08 g benzoic acid in 78 mL of the mixture of DMF and deionized water (V:V=12:1) were dissolved in a 100 mL capped vial. After that, the solution was sonicated for 10 min.

The vial was heated at 90 °C under stirring and kept the reaction for 6 h. The resulting purple nanosheets were washed twice with anhydrous ethanol and collected by vacuum filtration. Finally, the obtained Co-TCPP MOF powders were redispersed in 10 mL of ethanol.

S6.2 Synthesis of Co-TCPP/$Ti_3C_2T_x$-20

Co-TCPP(Fe)/$Ti_3C_2T_x$-20 hybrid was prepared through an ultrasound-assisted method.

First, 1 mL of 20 mg/mL Co-TCPP suspension in ethanol solution and 5 mL of 0.2 mg/mL $Ti_3C_2T_x$ aqueous solution were added to a 10 mL glass bottle. Then, the mixture was sonicated for 10 min and the product was heated under vacuum at 30 °C for 30 minutes and then stored under nitrogen atmosphere. The mass ratio of Co-TCPP to $Ti_3C_2T_x$ was 20 to 1.

S6.3 The Sensing Performance of Co-TCPP/$Ti_3C_2T_x$ Based Sensor

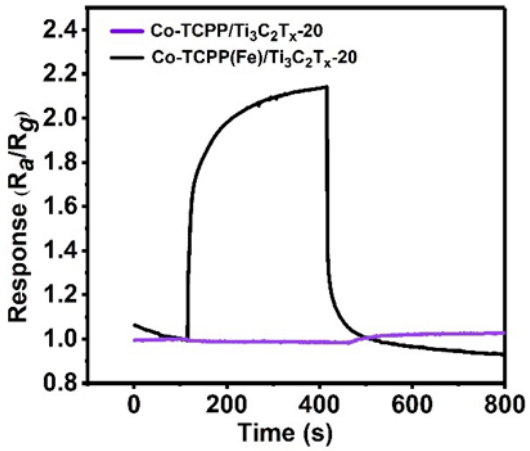

Figure S6 Gas sensing responses of Co-TCPP/$Ti_3C_2T_x$-20 based sensor and Co-TCPP(Fe)/$Ti_3C_2T_x$-20 based sensor toward 10 ppm NO at room temperature.